J. Gen. Appl. Microbiol., **61**, 217–223 (2015)
doi 10.2323/jgam.61.217

jGAM

Full Paper

Expression and characterization of an *N*-oxygenase from *Rhodococcus jostii* RHAI

(Received June 8, 2015; Accepted July 28, 2015)

Karl J. Indest,* Jed O. Eberly, and Dawn E. Hancock

U.S. Army Engineer Research and Development Center, Environmental Laboratory, Vicksburg, MS 39180, U.S.A.

Nitro group-containing natural products are rare in nature. There are few examples of *N*-oxygenases, enzymes that incorporate atmospheric oxygen into primary and secondary amines, characterized in the literature. *N*-oxygenases have yet to be characterized from the *Corynebacterineae*, a metabolically diverse group of organisms that includes the genera *Rhodococcus*, *Gordonia*, and *Mycobacterium*. A preliminary *in silico* search for *N*-oxygenase AurF gene orthologs revealed multiple protein candidates present in the genome of the Actinomycete *Rhodococcus jostii* RHAI (RHAI_ro06104). Towards the goal of identifying novel biocatalysts with potential utility for the biosynthesis of nitroaromatics, AurF ortholog RHAI_ro6104 was cloned, expressed and purified in *E. coli* and amine and nitro containing phenol substrates tested for activity. RHAI-ro06104 showed the highest activity with 4-aminophenol, producing a V_{max} of 18.76 μM s^{-1} and a K_m of 15.29 mM and demonstrated significant activities with 2-aminophenol and 2-amino-5-methylphenol, producing a V_{max} of 12.86 and 12.72 μM s^{-1} with a K_m of 8.34 and 2.81 mM, respectively. These findings are consistent with a substrate range observed in other *N*-oxygenases, which seem to accommodate substrates that lack halogenated substitutions and side groups directly flanking the amine group. Attempts to identify modulators of RHAI-ro06104 gene activity demonstrated that aromatic amino acids inhibit expression by almost 50%.

Key Words: aromatic amino acids; *N*-oxygenase; *Rhodococcus*

Introduction

Nitro group-containing natural products are relatively rare in nature with fewer than 200 known examples. These compounds have been isolated from various biological sources including plants, fungi, bacteria, and mammals, and display a wide range of structural diversity (Ju and Parales, 2010; Parry et al., 2011; Winkler and Hertweck, 2007). As a result of this structural diversity, these compounds exhibit an array of biological activities including antibiotic, antitumor, and cell signaling properties. In contrast, synthetically manufactured nitro compounds such as those found in pharmaceuticals, dyes, and energetic compounds are relatively common and their synthesis often generates intermediates and/or end products that are environmentally unfriendly. For example, the manufacture of nitroaromatic explosives such as 2,4,6-trinitrotoluene (TNT) yields a number of partially nitrated compounds along with the desired TNT. Most of these nitroaromatic compounds are potentially more toxic than TNT itself (Rickert et al., 1984). Likewise, the manufacture of hexahydro-1,3-5-trinitro-1,3,5-triazine (RDX) requires hexamine as a starting material, a compound that easily decomposes to the known carcinogen formaldehyde, and large amounts of concentrated nitric acid (Bachmann and Sheehan, 1949). The discovery of enzymatic catalysts capable of incorporation of molecular oxygen directly into amines offers a potential green biosynthesis route for nitro group-containing compounds.

Multiple mechanisms are possible for the biotic formation of nitro compounds: nitration, and oxygenation of amine containing compounds. While direct nitration of aromatic compounds is a well known synthetic reaction, evidence suggests that the formation of some antibiotics and alkaloids are naturally produced by this pathway (Winkler and Hertweck, 2007). Studies in Gram positive

*Corresponding author: Karl J. Indest, CEERD EP-P, U.S. Army Engineer Research and Development Center, 3909 Halls Ferry Road, Vicksburg, MS 39180, U.S.A.
Phone: (601) 634-2366 Fax: (601) 634-4017 E-mail: Karl.J.Indest@usace.army.mil

None of the authors of this manuscript has any financial or personal relationship with other people or organizations that could inappropriately influence their work.

bacteria indicate that nitric oxide synthase activity may also be directly involved in the nitration reaction (Kers et al., 2004; Winkler and Hertweck, 2007). Aromatic nitro containing compounds can also result from the enzymatic oxidation of an amine group (Winkler and Hertweck, 2007). Relatively little is known about enzymatic *N*-oxygenation of aromatic amines to nitroaromatics, despite the fact that enzymatic reduction of nitroaromatic compounds is prevalent in the explosives biodegradation literature (Crocker et al., 2006; Ju and Parales, 2010).

Few examples of *N*-oxygenases, oxygenases that directly incorporate molecular oxygen into primary and secondary amines, have been characterized. AurF and PrnD were the first examples of *N*-oxygenases described, each of which are involved in the biosynthesis of aureothin and pyrrolnitrin, respectively (Choi et al., 2008; He et al., 2001; Kirner et al., 1998; Krebs et al., 2007; Lee et al., 2005; Simurdiak et al., 2006; Zhang and Parry, 2007). AurF catalyzes the formation of *p*-nitrobenzoate from *p*-aminobenzoate, an unusual component of the aureothin polyketide synthase. There have been conflicting reports regarding the structure of AurF, some suggesting the active site contains diiron while others suggesting an iron and manganese complex (Krebs et al., 2007; Winkler et al., 2007; Zocher et al., 2007). While some structural and biochemical data suggest that AurF may employ a binuclear manganese center, Choi et al. (2008) indicated that a diiron center is more likely in the *Streptomyces thioluteus* AurF. In contrast, PrnD is a Rieske mononuclear non-heme enzyme that catalyzes the oxidation of the amino group of aminopyrrolnitrin to a nitro group, forming pyrrolnitrin. These enzymes were initially characterized from *S. thioluteus*, in the case of AurF, and *Pseudomonas fluorescens*, in the case of PrnD. More recently, other putative *N*-oxygenases have been characterized, FrbG (Johannes et al., 2010), CmlI (Lu et al., 2012; Makris et al., 2010) and PsAAO (Platter et al., 2011). The few enzymes characterized thus far have demonstrated limited substrate specificities with a preference for *p*-aminobenzoates and *o*-aminophenols (Platter et al., 2011; Winkler et al., 2006).

Thus far, *N*-oxygenases have yet to be characterized from the *Corynebacterineae*, a metabolically diverse group of organisms that includes the genera *Rhodococcus*, *Gordonia*, and *Mycobacterium*. A preliminary *in silico* search for putative *N*-oxygenase AurF gene orthologs present in *Rhodococcus jostii* RHAI revealed multiple putative protein candidates (McLeod et al., 2006). Towards the goal of identifying novel biocatalysts with a potential utility for the biosynthesis of nitroaromatics, AurF ortholog RHAI_ro06104 (E value 10^{-48}) was codon-optimized, cloned, expressed, and purified in *E. coli* and a range of possible amine and nitro containing phenol substrates tested for activity.

Materials and Methods

Bacterial strains and culturing conditions. Overnight cultures of *Rhodococcus jostii* RHAI were routinely grown on Luria Bertani (LB) medium diluted to 30% and incubated at 30°C, with shaking at 180 rpm. Pre-stationary phase *R. jostii* RHAI cells were induced for 1 h in the presence of 1) 5 mM shikimic acid, 2) 1 mM para amino benzoic acid (PABA), 3) 3 mM aromatic amino acid mix consisting of phenylalanine (F), tryptophan (Y) and tyrosine (W), and 4) media only without supplements as a negative control. Following induction, cells were incubated for 6–8 h and then subjected to real-time qPCR analysis to measure induction of putative *N*-oxygenase RHAI-ro06104. All studies were done in 50 ml of base medium in 250 ml flasks. Recombinant *E. coli* BL21StarDE3 (Life Technologies, Grand Island, NY) cultures were maintained in LB culture media in the presence of kanamycin at a concentration of 50 μg/ml.

Table 1. Substrates tested in this study and their associated molar extinction coefficients.

Substrate	ε ($M^{-1}cm^{1}$)	Wavelength (nm)
2-aminophenol	17.4	410
4-aminophenol	85.9	410
2-amino-5-methylphenol	123	418
2-amino-4-nitrophenol	n.d.	360
5-amino-2-methoxyphenol	4110	418
2-amino-5-chlorophenol	340	410

RNA extraction and real-time PCR analysis. Total RNA was extracted from *R. jostii* RHAI cells using the Qiagen RNeasy kit (Qiagen, Valencia, CA). Prior to extraction, an enzymatic lysis/mechanical disruption step was added to the protocol, whereby the cell pellet was re-suspended in 100 μl TE buffer and 200 μl lysozyme (20 mg ml^{-1}), transferred to a MP Biomedicals Lysing Matrix B tube (MP Biomedicals, Santa Ana, CA) and disrupted in an MP Biomedicals FastPrep24 for 30 s at 6 M s^{-1}. An optional on-column DNA digestion using the Qiagen RNase-Free DNase Kit was performed to remove any remaining DNA. The quantity and quality of RNA was assessed with the Agilent 2100 Bioanalyzer using the Agilent RNA 6000 Kit (Agilent, Santa Clara, CA). qPCR Reactions were performed using an Applied Biosystems 7900HT system. PCR was carried out in 20 μl reaction volumes containing 0.25 μmol primers (primers RHAI_ro06104f, TGACGGTGGCGGAGATCT and RHAI_ro06104r, CGGCTGGATGACGTCGTT for RHAI-ro06104 and primers RHAIsigA_F, GGCGTGATGTCCATTTCCTT and RHAIsigA_R, CATGGTGGAGGTCATCAACAAG for *sigA* from RHAI (Zhu et al., 2015)) and 60 ng of cDNA template using the Invitrogen 2X Power SYBR master mix. Amplification conditions for this reaction consisted of a single step at 95°C for 10 min followed by 40 cycles at 95°C for 15 s and 60°C for 1 min. Data were analyzed using the accompanying Applied Biosystems 7900HT analysis software to generate relative gene expression values across the growth conditions tested based on "delta delta Ct" values (Livak and Schmittgen, 2001) using the *sigA* from *R. jostii* RHAI as an endogenous control (Zhu et al., 2015).

N-oxygenase protein purification and activity assay. A 957 bp fragment representing a 35.9 kDa putative *N*-oxygenase protein encoded by RHAI-ro06104 was codon optimized for expression in *E. coli* and synthesized (Celtek

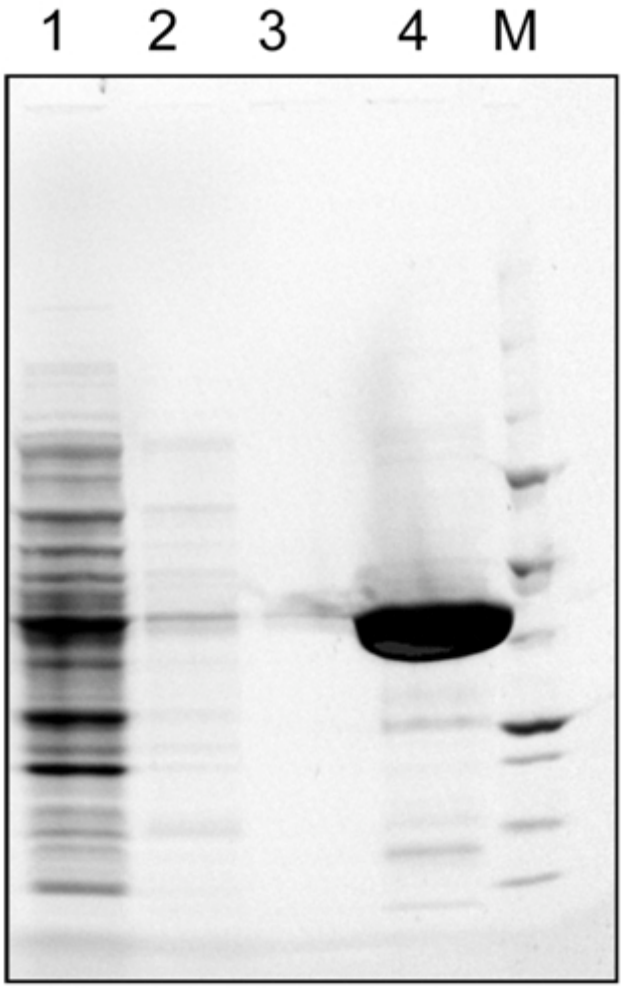

Fig. 1. SDS-PAGE analysis of the recombinant protein RHAI-ro06104. Proteins recovered at different purification steps were separated by SDS 20% polyacrylamide gel electrophoresis. Lane 1: cleared cell lysate, lanes 2–3: column washes, lanes 4: eluted protein, lane M: BioRad Precision Plus protein standards 250, 150, 100, 75 (bold), 50 (bold), 37, 25 (bold), 20, and 10 kDa from the top.

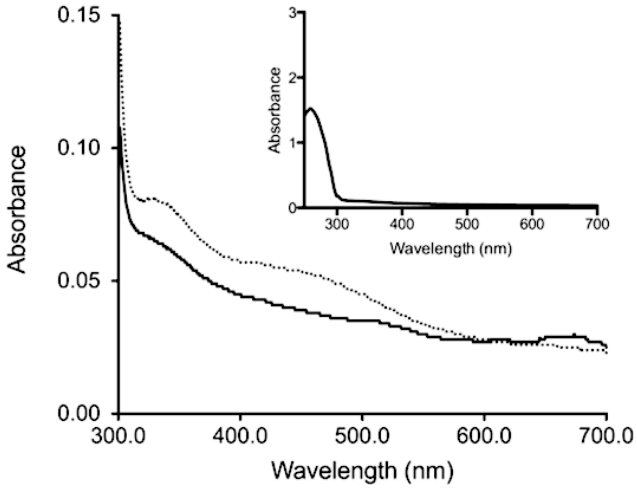

Fig. 2. Absorption spectra of the putative *N*-oxygenase from *R. jostii*. Solid line and inset: Absorption spectra of purified Rha1-ro06104. Dashed line: Absorption spectra of Rha1-ro06104 upon addition of 0.8 M sodium azide.

Biosciences) in the pGH vector incorporating flanking EcoRI restriction sites (Invitrogen, Carlsbad, CA). The EcoRI fragment containing RHAI-ro06104 was liberated from the pGH vector via EcoRI restriction enzyme digestion, gel purified with a Wizard SV Gel and PCR Cleanup System kit (Promega, Madison, WI), and cloned into the EcoRI site of the pASK-IBA5plus protein expression vector (IBA Life Sciences, Germany). Recombinant clones were transformed into *E. coli* One-Shot BL21StarDE3. Clones were sequenced using Invitrogen's BigDye Terminator v3.1 sequencing kit according to the manufacturer's instructions to confirm insert orientation and correct protein reading frame. Strep-TagII labeled RHAI-ro06104 protein, estimated at 38.1 kDa (339 amino acids), was expressed and purified according to the manufacturer's instructions using Strep-Tactin® Superflow columns (IBA Life Sciences, Germany). Briefly, a 20 ml culture of the RHAI-ro06104 containing *E. coli* clone was grown up overnight and added to 1 L of LB with 100 μg ml^{-1} ampicillin. Cultures were grown at 37°C to an OD_{600} of 0.5–0.6 then induced with 200 μg L^{-1} anhydrotetracycline (Sigma-Aldrich Corp., St. Louis, MO) in Dimethylformamide (DMF). One mM ferrous ammonium was added to ensure proper incorporation of iron in the enzyme active site. Following induction, the temperature was reduced to 30°C and cells were incubated with constant shaking for 3 h. Cells were harvested by centrifugation at 4000 × *g* for 10 min at 4°C. The cell lysate was prepared by three passages through a French Press (Glen Mills Model 11, Clifton, NJ) at 20,000 psi and all cell debris removed by centrifuging the lysate at 14,000 × *g*, 15 min at 4°C. Cleared lysates were loaded on Strep-Tactin® columns and the proteins were purified following the manufacturer's instructions. Purified proteins were concentrated using Millipore's Amicon ultra 30,000 MWCO filters.

Purified proteins were quantified via the Bradford assay, and analyzed on a Bio-Rad 4–20% Criterion Stain-Free Tris-HCl gel (Bio-Rad, Hecules, CA), after solubilizing in a 2x Laemmli Sample Buffer (Bio-Rad), to confirm the size and purity of the target protein. The absorption spectrum of the putative *N*-oxygenase was characterized as previously described (Makris et al., 2010; Platter et al., 2011). Briefly, the protein was diluted to a final concentration of 25 uM in a buffer containing 50 mM Tris, pH 7.5, 50 mM NaCl, and 5% glycerol. The UV-Vis spectrum was measured from 300–700 nm in the presence and absence of 0.8 M sodium azide. *N*-oxygenase activity for various aromatic amines (Table 1) was determined as described previously (Platter et al., 2011). Briefly, proteins were diluted to a final concentration of 50 μM protein in IBA buffer E, 25 mM NaCl, 1.5% H_2O_2, 40% MeOH, and a 0.1–150 mM substrate range. The molar extinction coefficient (ε) for each substrate was determined (Platter et al., 2011) (Table 1). Absorbance data was measured and collected for 10 min at wavelengths determined from the extinction coefficients. Enzyme-free controls were used to account for the spontaneous oxidation of the aromatic amine substrates under the same assay conditions and subtracted as background. All reactions were carried out in

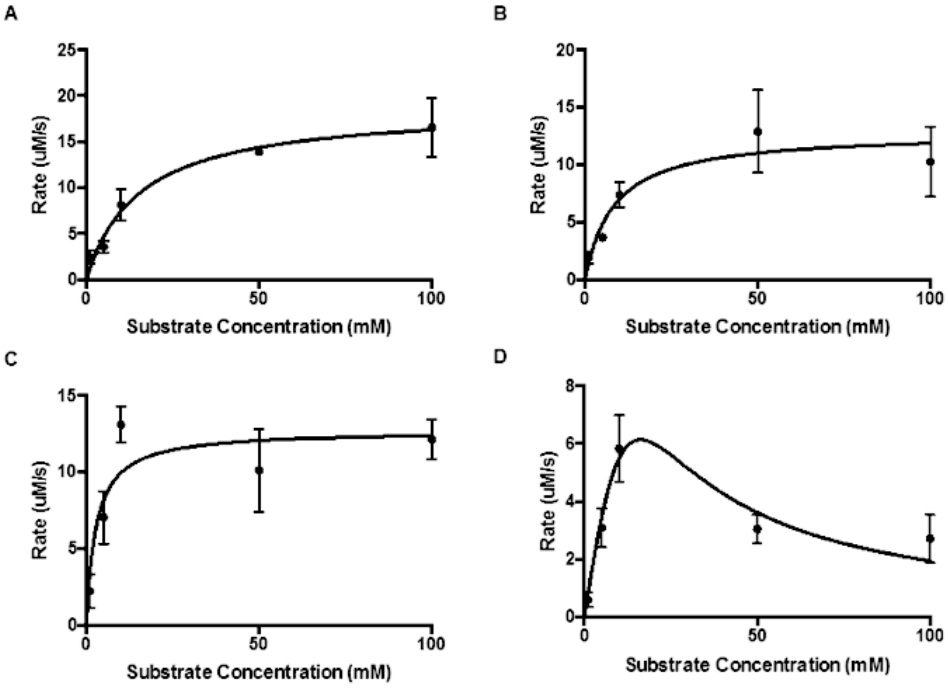

Fig. 3. Michaelis-Menten kinetics of RHAI-ro06104 in the presence of 4-aminophenol (A), 2-aminophenol (B), 2-amino-5-methylphenol (C), and 2-amino-4-methylphenol (D). The black line is a nonlinear fit of the data.

Table 2. Michaelis-Menten kinetics for RHAI-ro06104 and the tested substrates.

Substrate	K_m (mM)	V_{max} (uM/s)	K_{cat} (s^{-1})
4-aminophenol	15.29	18.76	0.38
2-aminophenol	8.34	12.86	0.26
2-amino-5-methylphenol	2.81	12.72	0.25
2-amino-4-methylphenol	1.42	3.86	0.08

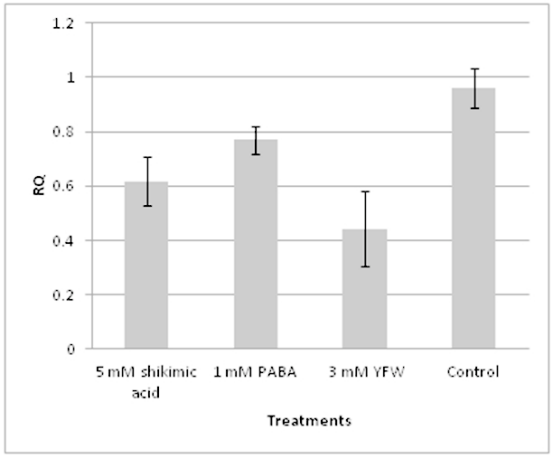

Fig. 4. Quantitative real-time PCR expression analysis of RNA harvested from RhaI cells grown for 8 h on media containing 5 mM shikimic acid, 1 mM para amino benzoic acid (PABA), 3 mM aromatic amino acid mix consisting of phenylalanine (F), tryptophan (Y) and tyrosine (W), and media only without supplements as a negative control.

96-well plates and analyzed using a UV-vis spectrophotometer plate reader (BioTeK, Winooski, VT). Initial rates were determined from the most linear region of the spectra as previously described (Platter et al., 2011) and the data were fit to a Michaelis-Menten model with and without substrate inhibition. The Michaelis-Menten kinetic parameters for substrate concentration at 1/2 maximum activity (K_m), maximum enzyme activity (V_{max}), and enzyme turnover (K_{cat}) were determined by nonlinear regression using GraphPad Prism version 6.0, (GraphPad Software, La Jolla California).

Results

Expression and characterization of RHAI-ro06104

The *N*-oxygenase enzyme encoded by RHAI-ro06104 was cloned, heterologously expressed and purified. A prominent expected band of ~38 kDa was observed when the sample was electrophoresed through a 4–20% SDS-PAGE gel (Fig. 1). The addition of 0.8 M sodium azide to the protein resulted in a shift in the UV-Vis spectrum with broad absorption bands at 345 and 450 nm (Fig. 2). These absorbance features are consistent with the formation of azide complexes formed by other proteins containing oxo-bridged diiron clusters (Fox et al., 1993; Makris et al., 2010). *N*-oxygenase activity for various aromatic amines (Table 1) was determined as described previously (Platter et al., 2011) using 1.5% hydrogen peroxide as an electron donor. Enzyme activity was monitored spectrophotometrically resulting in a best fit with a conventional Michaelis-Menten model, indicating there was no substrate inhibition with most substrates tested (Fig. 3). The only exception to this was 2-amino-4-methylphenol, which appeared to be inhibitory at concentrations of 20 mM and higher (Fig. 3D). Of the substrates tested in Table 1, RHAI-ro06104 showed the highest activity with 4-aminophenol,

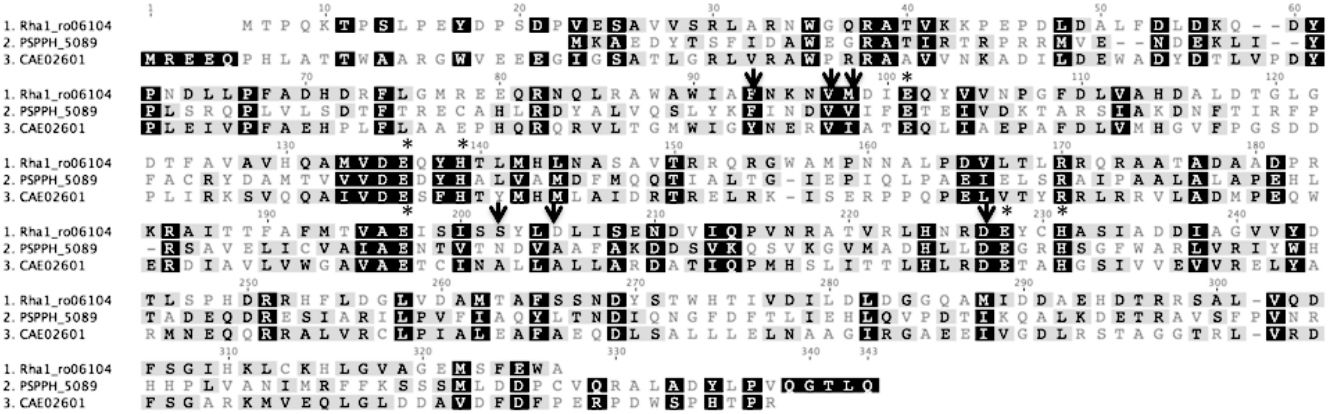

Fig. 5. Protein sequence alignment of AurF orthologs that have been functional characterized from *S. thioluteus* (CAE02601), *P.* pv *phaseolicola* (PSPPH_5089), and *R. jostii* RHAI (RHAI_ro06104).

The characteristic iron binding EX29DEX2H motif is highlighted with an asterisk and residues believed to comprise the active site pocket are marked with downward pointing arrows.

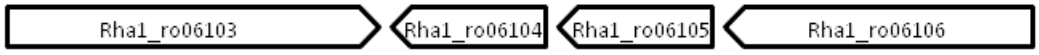

Fig. 6. Genomic context in which the *N*-oxygenase Rha1_ro06104 resides.

The putative *N*-oxygenase Rha1-ro06104 is located directly down-stream of a nonribosomal peptide synthetase (Rha1-ro06103) and directly upstream of a bifunctional chorimate mutase/prephenate dehydrogenase (Rha1-ro06105), and a bifunctional anthranilate synthase component I/II (Rha1-ro06106).

producing a V_{max} of 18.76 μM s^{-1} and K_m of 15.29 mM (Table 2). RHAI-ro06104 also demonstrated significant activities with substrates 2-aminophenol and 2-amino-5-methylphenol, producing a V_{max} of 12.86 and 12.72 μM s^{-1} with a K_ms of 8.34 and 2.81 mM, respectively. RHAI-ro06104 demonstrated little activity towards 2-amino-4-nitrophenol producing a marginal V_{max} of 3.86 μM s^{-1} with a K_m of 1.42 mM. The remaining substrates presented in Table 1 showed no transformation in the presence of RHAI-ro06104. RHAI-ro06104 was also tested with 4-aminobenzoic acid (PABA), which is the natural substrate for AurF *N*-oxygenases (He et al., 2001). Activity was only observed with substrate concentrations of 10 mM or less. At higher concentrations a precipitate formed due to the low solubility of PABA in an aqueous solution. Maximum activity with PABA was 2.61 μM s^{-1} (data not shown).

No activity was observed with halogenated side groups such as 2-amino-4-chlorophenol and 2-amino-5-chlorophenol or side groups that directly flanked the amino group, such as 2-amino-3-methylphenol and 2-amino-5-nitrophenol (data not shown).

Effects of small molecules on expression of RHAI-ro06104

The putative *N*-oxygenase RHAI-ro06104 is located directly downstream of a biofunctional chorimate mutase/prephenate dehydrogenase (RHAI-ro06105) and a bifunctional anthranilate synthase component I/II (RHAI-ro06106), all of which are oriented in the same direction. These upstream genes carry out the first steps in the parallel biosynthetic pathways for the aromatic amino acids phenylalanine (F), tryptophan (Y) and tyrosine (W), as well as PABA. As a result, the possibility exists that these molecules may influence RHAI-ro06104 gene expression. Real-time PCR analysis of RHAI-ro06104 extracted from RHAI cells in an early stationary phase grown in a rich medium confirmed expression of this putative gene (Fig. 4), indicating it was not a silent cryptic gene. Attempts to identify modulators of gene activity revealed that a mixture of aromatic amino acids inhibited expression of this gene by almost 50% (Fig. 4). PABA, the putative natural substrate for AurF, and shikimic acid also caused a 25% and 40% decrease in expression of RHAI-ro06104, respectively.

Discussion

Towards the goal of identifying novel biocatalysts with a potential utility for the biosynthesis of nitroaromatic containing energetics, an AurF ortholog from *R. jostii* was cloned and expressed in *E. coli* and a range of possible amine substrates tested for activity. UV-vis spectra of oxidized RHAI-ro06104 from *R. jostii* RHA1 showed broad absorption bands at 345 and 450 nm. These absorption bands indicate the formation of a chromophore, which is observed for azide complexes in other proteins containing oxo-bridged diiron centers (Makris et al., 2010). The presence of the iron-azide charge transfer band at around 450 nm is consistent with reports of other diiron monooxygenases (Fox et al., 1993; Makris et al., 2010). Substrate activity assays with Rha1-ro06104 were consistent with a substrate range, which favored ortho and para-regioselective oxygenation of aromatic amines. The addition of strong electron withdrawing side groups at the 4′ and 5′ positions of 2-aminophenol resulted in poor substrates for oxygenation of the 2′ amine group. Activity

was observed with methyl groups in the para and meta positions but not in the ortho position, presumably due to steric hindrance. Most substrates, with the exception of 2-amino-4-methylphenol, did not appear to have an inhibitory effect on the enzyme based on the Michaelis-Menten fit of the data (Fig. 3). In contrast, substrate inhibition was observed with multiple substrates with PsAAO but not with 2-amino-4-methylphenol (Platter et al., 2011).

In general, RHAI-ro06104 showed no activity with halogenated side groups as well as side groups directly flanking the amine group (data not shown). The ability of functional groups on the substrates tested to donate and/or remove electrons from the aromatic ring likely dictate RHAI-ro06104 activity with halogens being weakly deactivating (electron withdrawing) compared to electron donating functional groups, i.e. -OH, -OR, $-NH_2$, and $-NH_R$. The ring positions of side groups may also have inhibited enzyme activity as a result of steric hindrance in the case of 2-amino-3-methylphenol and 5-amino-2-methoxyphenol.

RHAI-ro06104 also showed greater activity with aminophenol derivatives than with PABA, the putative natural substrate for RHAI-ro06104. This is similar to what was reported from PsAAO, the *N*-oxygenase ortholog, from *Pseudomonas syringae* pv. *Phaseolicola* (Platter et al., 2011). The K_{cat} value for 4-aminophenol was 0.38 s^{-1} (Table 2) which was the same that was reported for PsAAO, however RHAI-ro06104 showed activity with fewer substrates than PsAAO or AurF. RHAI-ro06104 did not exhibit strong para regioselectivity compared to AurF (Winkler et al., 2006). Activity was observed with both para and ortho hydroxyl groups (4 and 2-aminophenol, respectively). Interestingly, activity was only observed with hydroxyl-substituted arylamines. This is similar to PsAAO, which showed activity primarily with aminophenols and only a few PABA derivatives (Platter et al., 2011). In contrast, AurF showed activity with a broad range of PABA analogues (Winkler et al., 2006). An inspection of a protein alignment amongst the three proteins revealed that the characteristic iron binding EX28-33DEX2H motif (Krebs et al., 2007) is present in RHAI-ro06104. Analysis of the crystal structure of the AurF protein (PDB ID: 3CHH_B) from *S. thioluteus* (Choi et al., 2008) indicates that the amino acids in this binding motif at positions 200–202 are closely associated with the diiron center. The residues believed to comprise the active site pocket showed amino acid substitutions that were conserved based on similar side chain chemistries (Fig. 5). These substitutions may have influenced substrate specificity as in the case of the substitution of a serine for an aspargine or threonine at position 201 in RHAI_ro06104.

The larger genome context in which Rha1-ro06104 resides suggests it may be a component of a secondary metabolic gene cluster, although the secondary metabolite produced by this gene cluster is not known (Fig. 6). Directly downstream of this gene in the opposite orientation is a large predicted nonribosomal peptide synthetase (NRPS), Rha1-ro06103. Directly upstream of RHAI-ro06104 are genes encoding for a biofunctional chorimate mutase/prephenate dehydrogenase (RHAI-ro06105) and a bifunctional anthranilate synthase component I/II (RHAI-ro06106), all of which are oriented in the same direction. These enzymes are components of the shikimate pathway responsible for the biosynthesis of PABA (the putative natural substrate for AurF (He et al., 2001) and the aromatic amino acids, phenylalanine, tryptophan and tyrosine. In this context, the collocation of RHAI-ro06104, RHAI-ro06105 and RHAI-ro06106 suggest that aromatic amines along with PABA may be substrates for *N*-oxygenation. This is consistent with our observation that aminophenol derivatives are the preferred substrates for RHAI-ro06104. Therefore, we hypothesized that PABA and the aromatic amino acids phenylalanine, tyrosine, and tryptophan may modulate RHAI-ro06104 gene expression. Attempts to modulate expression of RHAI-ro06104 in the presence of shikimic acid, PABA, and aromatic amino acids resulted in the inhibition of gene expression (Fig. 4).

Currently, chemical synthesis of nitroaromatics involves the use of strong acids and results in multiple toxic chemical byproducts. Biological starter molecules in combination with enzymatic catalysts offer a green alternative to chemical nitroaromatic biosynthesis. There has been interest in aminobenzoates as natural building blocks for new chemicals (Walsh et al., 2012). Chorismate biochemistry offers an excellent starting point for the synthesis of nitroaromatics. The addition of an amine group to the chorismate aromatic ring can be accomplished via sequential biologically catalyzed transamination reactions to yield a suitable aromatic amine substrate for *N*-oxygenation. Subjecting the enzymes in this pathway to modern protein engineering and directed evolution methods has the potential to customize substrate specificity, ultimately leading to new green synthesis pathways for nitroaromatics based on chorismate biochemistry.

Acknowledgments

This research was funded through the US Army Corps of Engineers Environmental Quality Program. Views, opinions and/or findings contained herein are those of the authors and should not be construed as an official Department of the Army position or decision, unless so designated by other official documentation.

References

Bachmann, W. E. and Sheehan, J. C. (1949) A new method of preparing the high explosive RDX. *J. Am. Chem. Soc.*, **71**, 1842–1845

Choi, Y. S., Zhang, H., Brunzelle, J. S., Nair, S. K., and Zhao, H. (2008) In vitro reconstitution and crystal structure of *p*-aminobenzoate *N*-oxygenase (AurF) involved in aureothin biosynthesis. *Proc. Natl. Acad. Sci. USA*, **105**, 6858–6863.

Crocker, F. H., Indest, K. J., and Fredrickson, H. L. (2006) Biodegradation of the cyclic nitramine explosives RDX, HMX, and CL-20. *Appl. Microbiol. Biotechnol.*, **73**, 274–290.

Fox, B. G., Shanklin, J., Somerville, C., and Münck, E. (1993) Stearoyl-acyl carrier protein delta 9 desaturase from *Ricinus communis* is a diiron-oxo protein. *Proc. Natl. Acad. Sci. USA*, **90**, 2486–2490.

He, J., Magarvey, N., Piraee, M., and Vining, L. C. (2001) The gene cluster for chloramphenicol biosynthesis in Streptomyces venezuelae ISP5230 includes novel shikimate pathway homologues and a monomodular non-ribosomal peptide synthetase gene. *Microbiology*, **147**, 2817–2829.

Johannes, T. W., DeSieno, M. A., Griffin, B. M., Thomas, P. M., Kelleher, N. L. et al. (2010) Deciphering the late biosynthetic steps of antimalarial compound FR-900098. *Chem. Biol.*, **17**, 57–64.

Ju, K. S. and Parales, R. E. (2010) Nitroaromatic compounds, from synthesis to biodegradation. *Microbiol. Mol. Biol. Rev.*, **74**, 250–272.

Kers, J. A., Wach, M. J., Krasnoff, S. B., Widom, J., Cameron, K. D. et al. (2004) Nitration of a peptide phytotoxin by bacterial nitric oxide synthase. *Nature*, **429**, 79–82.

Kirner, S., Hammer, P. E., Hill, D. S., Altmann, A., Fischer, I. et al. (1998) Functions encoded by pyrrolnitrin biosynthetic genes from *Pseudomonas fluorescens*. *J. Bacteriol.*, **180**, 1939–1943.

Krebs, C., Matthews, M. L., Jiang, W., and Bollinger, J. M. (2007) AurF from *Streptomyces thioluteus* and a possible new family of manganese/iron oxygenases. *Biochemistry*, **46**, 10413–10418.

Lee, J., Simurdiak, M., and Zhao, H. (2005) Reconstitution and characterization of aminopyrrolnitrin oxygenase, a Rieske *N*-oxygenase that catalyzes unusual arylamine oxidation. *J. Biol. Chem.*, **280**, 36719–36728.

Livak, K. J. and Schmittgen, T. D. (2001) Analysis of relative gene expression data using real-time quantitative PCR and the 2(-Delta Delta C(T)) method. *Methods*, **25**, 402–408.

Lu, H., Chanco, E., and Zhao, H. (2012) CmlI is an -oxygenase in the biosynthesis of chloramphenicol. *Tetrahedron*, **68**, 7651–7654.

Makris, T. M., Chakrabarti, M., Munck, E., and Lipscomb, J. D. (2010) A family of diiron monooxygenases catalyzing amino acid beta-hydroxylation in antibiotic biosynthesis. *Proc. Natl. Acad. Sci. USA*, **107**, 15391–15396.

McLeod, M. P., Warren, R. L., Hsiao, W. W., Araki, N., Myhre, M. et al. (2006) The complete genome of *Rhodococcus* sp. RHA1 provides insights into a catabolic powerhouse. *Proc. Natl. Acad. Sci. USA*, **103**, 15582–15587.

Parry, R., Nishino, S., and Spain, J. (2011) Naturally-occurring nitro compounds. *Nat. Prod. Rep.*, **28**, 152–167.

Platter, E., Lawson, M., Marsh, C., and Sazinsky, M. H. (2011) Characterization of a non-ribosomal peptide synthetase-associated diiron arylamine *N*-oxygenase from *Pseudomonas syringae* pv. *phaseolicola*. *Arch. Biochem. Biophys.*, **508**, 39–45.

Rickert, D. E., Butterworth, B. E., and Popp, J. A. (1984) Dinitrotoluene: acute toxicity, oncogenicity, genotoxicity, and metabolism. *Crit. Rev. Toxicol.*, **13**, 217–234.

Simurdiak, M., Lee, J., and Zhao, H. (2006) A new class of arylamine oxygenases: evidence that *p*-aminobenzoate *N*-oxygenase (AurF) is a di-iron enzyme and further mechanistic studies. *Chembiochem.*, **7**, 1169–1172.

Walsh, C. T., Haynes, S. W., and Ames, B. D. (2012) Aminobenzoates as building blocks for natural product assembly lines. *Nat. Prod. Rep.*, **29**, 37–59.

Winkler, R. and Hertweck, C. (2007) Biosynthesis of nitro compounds. *Chembiochem.*, **8**, 973–977.

Winkler, R., Richter, M. E., Knupfer, U., Merten, D., and Hertweck, C. (2006) Regio- and chemoselective enzymatic *N*-oxygenation in vivo, in vitro, and in flow. *Angew. Chem. Int. Ed. Engl.*, **45**, 8016–8018.

Winkler, R., Zocher, G., Richter, I., Friedrich, T., Schulz, G. E. et al. (2007) A binuclear manganese cluster that catalyzes radical-mediated *N*-oxygenation. *Angew. Chem. Int. Ed. Engl.*, **46**, 8605–8608.

Zhang, X. and Parry, R. J. (2007) Cloning and characterization of the pyrrolomycin biosynthetic gene clusters from *Actinosporangium vitaminophilum* ATCC 31673 and *Streptomyces* sp. strain UC 11065. *Antimicrob. Agents Chemother.*, **51**, 946–957.

Zhu, S. H., Reuther, J., Liu, J., Crocker, F. H., Indest, K. J. et al. (2015) The essential role of nitrogen limitation in expression of xplA and degradation of hexahydro-1,3,5-trinitro-1,3,5-triazine (RDX) in *Gordonia* sp. strain KTR9. *Appl. Microbiol. Biotechnol.*, **99**, 459–467.

Zocher, G., Winkler, R., Hertweck, C., and Schulz, G. E. (2007) Structure and action of the *N*-oxygenase AurF from *Streptomyces thioluteus*. *J. Mol. Biol.*, **373**, 65–74.